Science of the Total Environment 699 (2020) 134387

Contents lists available at ScienceDirect

Science of the Total Environment

journal homepage: www.elsevier.com/locate/scitotenv

The fate of silver nanoparticles in riverbank filtration systems — The role of biological components and flow velocity

Laura Degenkolb [a,b,*,1], Frederic Leuther [c,1], Simon Lüderwald [d], Allan Philippe [e], George Metreveli [e], Sayed Amininejad [f], Hans-Jörg Vogel [c], Martin Kaupenjohann [a], Sondra Klitzke [b]

[a] Berlin University of Technology, Institute of Ecology, Department of Soil Science, Ernst-Reuter Platz 1, 10587 Berlin, Germany
[b] German Environment Agency, Section Drinking Water Treatment and Resource Protection, Schichauweg 58, 12307 Berlin, Germany
[c] Helmholtz Centre for Environmental Research Leipzig-Halle, Department of Soil System Science, Theodor-Lieser-Straße 4, 06120 Halle, Germany
[d] University of Koblenz-Landau, Institute for Environmental Sciences, Group of Ecotoxicology and Environment, Fortstraße 7, 76829 Landau, Germany
[e] University of Koblenz-Landau, Institute for Environmental Sciences, Group of Environmental and Soil Chemistry, Fortstraße 7, 76829 Landau, Germany
[f] Technical University of Munich, Institute of Hydrochemistry, Marchioninistr. 17, 81377 München, Germany

HIGHLIGHTS

- Outdoor & lab study: NP transport in absence and presence of biological components
- Biological components highly increase NP retention, independent of flow velocity.
- High NP retention under low flow velocity (<1 m d^{-1}) in lab and outdoor columns
- Experiment duration and flow rate increase NP mobility in near-natural systems.
- Strong NP attachment to biological components in riverbank filtration systems

GRAPHICAL ABSTRACT

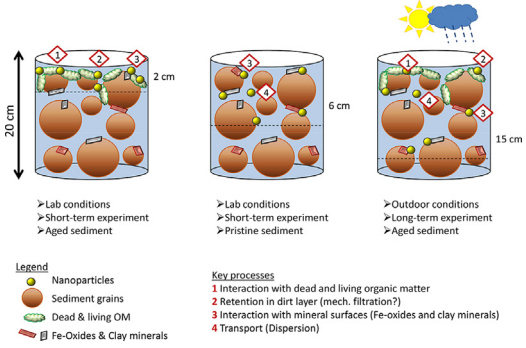

ARTICLE INFO

Article history:
Received 2 July 2019
Received in revised form 8 September 2019
Accepted 8 September 2019
Available online 10 September 2019

Editor: Damia Barcelo

Keywords:
Nanomaterial
Long-term experiment
Water-saturated transport
Near-natural condition
Biological retention
Mechanical filtration

ABSTRACT

Riverbank filtration is a natural process that may ensure the cleaning of surface water for producing drinking water. For silver nanoparticles (AgNP), physico-chemical interaction with sediment surfaces is one major retention mechanism. However, the effect of flow velocity and the importance of biological retention, such as AgNP attachment to biomass, are not well understood, yet.

We investigated AgNP (c = 0.6 mg L^{-1}) transport at different spatial and temporal scales in pristine and previously pond water-aged sediment columns. Transport of AgNP under near-natural conditions was studied in a long-term riverbank filtration experiment over the course of one month with changing flow scenarios (i.e. transport at 0.7 m d^{-1}, stagnation, and remobilization at 1.7 m d^{-1}). To elucidate retention processes, we conducted small-scale lab column experiments at low (0.2 m d^{-1}) and high (0.7 m d^{-1}) flow rate using pristine and aged sediments.

Overall, AgNP accumulated in the upper centimeters of the sediment both in lab and outdoor experiments. In the lab study, retention of AgNP by attachment to biological components was very effective under high and low flow rate with nearly complete NP accumulation in the upper 2 mm. When organic material was absent, abiotic filtration mechanisms led to NP retention in the upper 5 to 7 cm of the

* Corresponding author at: German Environment Agency, Section Drinking Water Treatment and Resource Protection, Schichauweg 58, 12307 Berlin, Germany
E-mail addresses: laura.degenkolb@campus.tu-berlin.de (L. Degenkolb), frederic.leuther@ufz.de (F. Leuther), luederwald@uni-landau.de (S. Lüderwald), philippe@uni-landau.de (A. Philippe), metreveli@uni-landau.de (G. Metreveli), s.amininejad@tum.de (S. Amininejad), hans-joerg.vogel@ufz.de (H.-J. Vogel), martin.kaupenjohann@tu-berlin.de (M. Kaupenjohann), Sondra.klitzke@uba.de (S. Klitzke).
[1] Both authors contributed equally.

https://doi.org/10.1016/j.scitotenv.2019.134387
0048-9697/

column. In the long-term study, AgNP were transported up to a depth of 25 cm. For the pristine sediment in the lab study and the outdoor experiments only erratic particle breakthrough was detected in a depth of 15 cm.

We conclude that physico-chemical interactions of AgNP with sediment surfaces are efficient in retaining AgNP. The presence of organic material provides additional retention sites which increase the filtration capacity of the system. Nevertheless, erratic breakthrough events might transport NP into deeper sediment layers.

1. Introduction

Riverbank filtration is an important process for drinking water production with the advantage of cleaning surface water by natural filtration mechanisms such as adsorption and degradation of anthropogenic pollutants. In Germany, about 16% of the drinking water is produced by managed aquifer recharge using bank filtration (Sprenger et al., 2017). Substances that can pass riverbank filtration systems may thus pose a risk for drinking water resources. The increasing use of silver nanoparticles (Ag NP) in industrial processes, medical products, textiles, and household appliances leads to an increasing release of Ag NP into the environment (Li et al., 2008; Tolaymat et al., 2010). For drinking water risk assessment, it is therefore important to investigate the transport of Ag NP in saturated sediments that act as natural filters for drinking water resources.

Since the early 2000s, NP fate and effects have been increasingly studied by many researchers (Fabrega et al., 2011; Sani-Kast et al., 2017). The risk for adverse effects of Ag NP to aquatic organisms was suggested by various studies (Andreï et al., 2016; Rajala et al., 2018; Ribeiro et al., 2017). Nanoparticle transport was mainly investigated in small-scale column experiments, using glass beads (Ben-Moshe et al., 2010 for metal oxide NP; Lecoanet and Wiesner, 2004 for fullerenes and metal oxide NP), quartz sand (Petosa et al., 2013 for CeO_2 NP), and soil columns (Cornelis et al., 2013; Sagee et al., 2012 for Ag NP). These experiments identified that the following physico-chemical filtration mechanisms dominate the transport and retention of NP:

(I) The extent of NP transport strongly depends on the hydrochemical *properties of the mobile phase*, such as pH, ionic strength, and natural organic matter (NOM) concentration. Increasing ionic strength leads to the compression of the electrical double layer of NP as well as of sediment grains of porous media. According to DLVO theory, this decreases repulsion forces between particles and collector surfaces and causes NP attachment and retention (Derjaguin and Landau, 1941). On the one hand, adsorption of NOM to NP surfaces leads to steric and electrostatic stabilization and may enhance NP mobility (i.e. Chen et al., 2012). On the other hand, the presence of multivalent cations may also reduce NP mobility by promoting NOM-NP flocculation (Kumahor et al., 2016; Philippe and Schaumann, 2014). As NOM is ubiquitous in the environment those organic molecules play an important role for NP fate in natural systems (Philippe and Schaumann, 2014).

(II) The physical *properties of the sediment system*, such as pore size distribution and flow velocity, have a strong impact on NP transport (e.g. Braun et al., 2015; Sagee et al., 2012). Due to the small size of NP, their mobility is strongly influenced by Brownian motion and, thus, diffusion. At low flow rates, NP mass transfer is dominated by diffusion to attachment sites (Adrian et al., 2018; Braun et al., 2015). Furthermore, low hydrodynamic shear forces reduce the probability of detachment (Metreveli et al., 2015). Therefore, NP retention increases with decreasing flow rate. However, most studies have been conducted at relatively high flow rates (ranging from 2.4 up to 55 m d^{-1} Darcy flux; Cornelis et al., 2013; El Badawy et al., 2013; Li et al., 2013; Lin et al., 2011; Petosa et al., 2013; Sagee et al., 2012; Sun et al., 2015; Taghavy et al., 2013) that might be unrealistic for saturated porous media (Kunkel and Wendland, 1997; Schubert, 2002). In these cases, high NP breakthrough was found. In contrast, flow rates below 1 m d^{-1} caused a very low Ag NP breakthrough in loamy sand in a study by Braun et al. (2015), but the effect of changing flow rates in the low flow range has not been studied so far.

(III) The *properties of the NP* themselves affect their interaction with the stationary phase and thus, their mobility. Although intrinsic properties of particles of different material lead to a wide range of NP surface charge and reactivity, organic capping agents prevent NP from aggregating. In pure quartz sand with a negative surface charge, the transport of citrate coated Ag NP follows the behavior of a conservative tracer while positively charged iron oxides or clay particles restrain citrate coated Ag NP (El Badawy et al., 2013). Thus, intrinsic NP properties might be masked by capping agents. Furthermore, increasing initial NP concentrations were found to enhance NP breakthrough as the limited number of attachment or straining sites becomes saturated at high NP concentrations (Bradford et al., 2006).

These retention mechanisms all focus on interactions of NP with the inorganic matrix of a saturated sediment system. However, biological surfaces such as biofilms, microorganisms, and detritus offer a high variety of potential attachment sites and can change the properties of the pore system (Hoffmann and Gunkel, 2011). In aquatic mesocosm experiments and transport studies a strong attachment of NP to biofilms and plants has been observed (Avellan et al., 2018; Nevius et al., 2012; Tripathi et al., 2012). Furthermore, aquatic sediments have been identified as important sinks for NP possibly due to biological surfaces (Geitner et al., 2018). Nevertheless, the role of biological structures in sediment systems is not taken into account in most column experiments and limits the transferability of lab results to natural systems.

In a previous study, we investigated the transport of citrate-coated Ag NP in the near-natural riverbank filtration system (Degenkolb et al., 2018) which is also used for the present experiments. Strong retention of Ag NP in the upper 10 cm of the column was observed which was explained by the low flow velocity (0.2 m d^{-1}) and the presence of biofilms and organic material without further exploration on these factors.

The present study aims at investigating the effect of different flow velocities and the presence of organic material on the retention and transport of Ag NP in saturated sediment systems based on the previous study. Therefore, the large-scale, long-term experiment was conducted with a higher flow velocity (0.7 m d^{-1}) than used in the previous study and changing flow scenarios (i.e. trans-

port at 0.7 m d^{-1}, stagnation, and remobilization at 1.7 m d^{-1}). Subsequently, we studied the importance of biological material (i.e. dead and living organic matter from biofilms, algae, and plants) on NP retention in lab column experiments by comparing the transport in pond water-aged and pristine sediments at low and high flow rate. The ecotoxicological relevance of NP transport behavior in near-natural sediment systems was verified by toxicity tests with the applied Ag NP as well as the effluents in different column depths. Hereby, the following two main hypotheses were tested:

I) The retention of Ag NP is strongly enhanced by NP attachment to biomass.
II) Increasing flow velocities increases transport and decreases retention of Ag NP in riverbank filtration systems.

2. Material and methods

2.1. Experimental design

To test the impact of organic retention mechanisms and flow velocity on Ag NP transport and retention in riverbank filtration systems, two kinds of experiments were performed: i) large-scale outdoor experiments with different flow velocities, i.e. 0.2 m d^{-1} (Degenkolb et al., 2018) and 0.7 m d^{-1}, and ii) laboratory column experiments with pristine and pond water-aged sediment for both flow rates. Fig. 1 provides an overview of the experimental design:

Transport of citrate-coated Ag NP was investigated in outdoor, near-natural riverbank filtration columns (length 1.5 m, surface area 1 m^2) imbedded in a slow sand filtration pond (a) over the course of one month. Within this time, a stagnation period (stopped flow) and a remobilization scenario (flow rate increased to 1.7 m d^{-1}) were included (b). The role of dead and living organic material on NP transport and retention was studied in lab-scale columns (c) using pristine (d) and pond water-aged sediments (e).

Both lab and outdoor columns were filled with coarse-grained medium sand (d_{50}: 0.38 mm, bulk density in the top 10 cm: 1.78 g cm^{-3}, size distribution see Fig. S1, provided by Sand + Kies Union GmbH, Hartmannsdorf), mainly containing quartz and trace amounts of several elements such as Fe (Fe_{tot}: 1.143 ± 0.094 g kg^{-1}), Al (Al_{tot}: 0.869 ± 0.135 g kg^{-1}), and Ti (observed by the EDX detector of the electron microscope, not quantified). As mobile phase, natural pond water diluted with reverse osmosis water to an electrical conductivity (EC) of 250–300 μS cm^{-1} was applied (Table 1).

2.2. Nanoparticle material

Citrate-coated, isotopically enriched ^{109}Ag NP with a hydrodynamic diameter of 48 ± 3 nm and a ζ-potential of −41 ± 3 mV were applied in all experiments. A detailed description of the preparation of ^{109}Ag NP can be found in Metreveli et al. (in prep). Briefly, metallic granulate of ^{109}Ag (99.67 ± 0.09% ^{109}Ag, STB Isotope Germany GmbH, Hamburg) was dissolved in concentrated nitric acid (HNO_3, 65%, Suprapur, Merck, Darmstadt) and heated in a water bath. After complete dissolution of the granulate, the solution was further heated until complete evaporation. The crystallized $AgNO_3$ was dissolved in deionized water, ultrafiltered (cut-off of 50 kDa), and adjusted to pH 4. To prepare ^{109}Ag NP, the method of Turkevich et al. (1951) modified for Ag was applied using $^{109}AgNO_3$ as described elsewhere (i.e. Klitzke et al., 2015).

The citrate coating was used to stabilize Ag NP suspensions against aggregation. For transport experiments, the ^{109}Ag NP were dispersed in diluted pond water to a final ^{109}Ag concentration of 0.61 ± 0.22 mg L^{-1} and a background concentration of Suwannee River (SR) NOM of 0.8 mg L^{-1} was adjusted. Stock solution of SR-NOM was prepared as described by Degenkolb et al. (2018). The mixtures were prepared 1 h prior to each column experiment to allow NP equilibration with SR-NOM.

The reader should note that NP suspensions of the outdoor and low flow lab experiment contained a second kind of NP, namely Ag@Au NP (i.e. Ag NP with a gold core, further information given in the Supporting Information and Fig. S2) with c_{NP} = 0.56 ± 0.26 - mg L^{-1} which were used to study the different transport of NOM-coated and uncoated Ag NP. However, due to poor recovery results it was not possible to analyze the data in a sufficient way. We assumed that interaction of both NP with each other was subsidiary as particle concentrations are very low resulting in a low collision frequency. In this manuscript, we show only the data of ^{109}Ag NP.

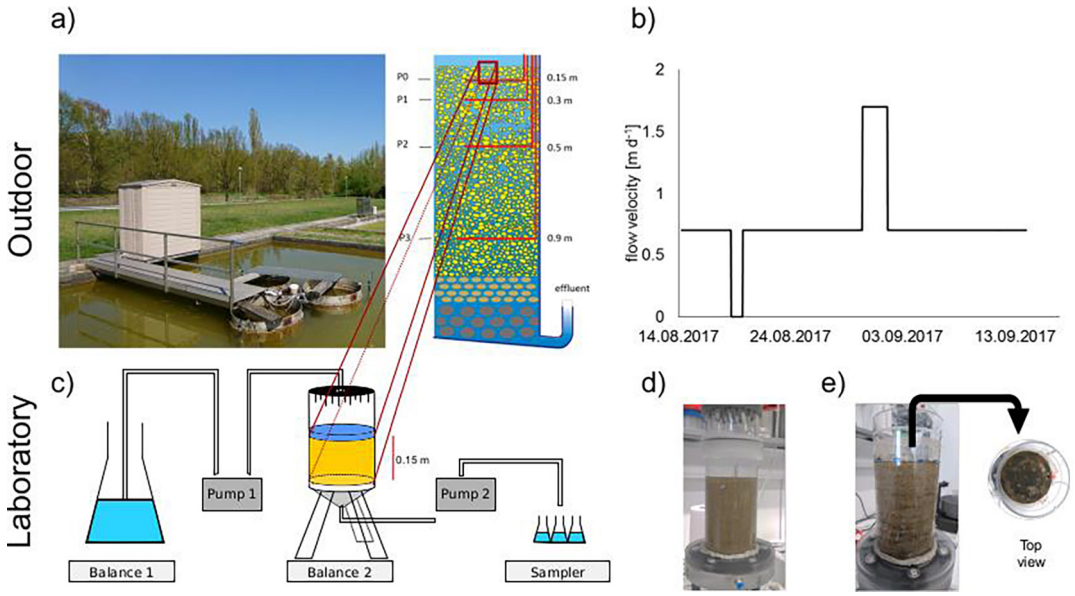

Fig. 1. Experimental design of the study where a) is the near-natural riverbank filtration system, surrounded of a slow sand filtration pond, b) the flow schedule of the outdoor experiment, c) the laboratory setup for the column experiments with pristine (d) and pond-aged sediment (e).

Table 1
Background ion and NP concentration of the mobile phase of lab and outdoor column experiments, mean and standard deviation (SD) of measurements of 3 replicates.

Elements/parameters	Lab experiment high flow		Lab experiment low flow		Outdoor column	
	Mean	SD	Mean	SD	Mean	SD
Ag NP [mg L^{-1}]	0.56	0.13	0.69	0.33	0.53	0.18
Al [mM]	b.d.l[a]		b.d.l[a]		b.d.l[a]	
Ca [mM]	0.781	0.011	0.678	0.004	0.563	0.012
Fe [mM]	b.d.l[a]		b.d.l[a]		0.111	0.012
K [mM]	0.001	0.001	0.023	0.000	0.030	0.002
Mg [mM]	0.171	0.002	0.157	0.001	0.140	0.001
Mn [mM]	b.d.l[a]		b.d.l[a]		0.039	0.011
Na [mM]	0.402	0.108	0.571	0.002	0.701	0.006
F^- [mM]	0.011	0.010	0.016	–	0.012	–
Cl^- [mM]	0.520	0.003	0.506	–	0.490	–
NO_3^- [mM]	0.016	0.014	0.012	–	0.003	–
SO_4^{2-} [mM]	0.507	0.002	0.503	–	0.453	–
TOC [mg L^{-1}]	4.1	0.5	5.1	2.3	5.3	0.2
EC [μS cm^{-1}]	262	14	297	0	257	8
pH	8.2	0.0	7.9	0.1	8.1	0.1

[a] Below detection limit.

2.3. Near-natural riverbank filtration experiment

To complement the low-flow experiment (0.2 m d^{-1}) conducted by Degenkolb et al. (2018), the transport and retention of Ag NP in a near-natural riverbank filtration system was investigated at a higher flow rate (0.7 m d^{-1}). For a detailed description of the column system, we refer readers to the previous publication (Degenkolb et al., 2018). In brief, two columns filled with pond water-aged sediments were included in a slow sand filtration pond. At a depth of 15, 30, 50, and 90 cm, sampling ports made of perforated stainless steel tubes were connected with PVC tubes to automatic sampling units; at the outflow water was sampled manually. The experiments were performed in duplicates for the duration of 1 month (14th August–13th September 2017).

The columns were fed by diluted natural pond water from the surrounding slow sand filtration pond which was mixed with reverse osmosis water to an EC of 250 μS cm^{-1} in a barrel before addition to sediment column. On top of the columns, a supernatant of 70 L was adjusted and hydrochemical parameters and ion concentrations (ICP-OES, iCAP 6000, Thermo Scientific and ion chromatography, DX-120, Dionex for cations and anions, respectively) were measured (Table 1). A tracer experiment in the columns was conducted 6 days before the start of the NP application (Fig. S3): NaCl solution was mixed in 70 L of column supernatant (EC = 1.37 mS cm^{-1}) and EC was measured in all 4 depths as well as in the outflow for detection of the tracer.

For the NP experiment, NP suspensions were added to 70 L of column supernatant. After infiltration of the NP-containing supernatant the columns were flushed with diluted pond water during the complete experimental period. A flow velocity of 0.7 m d^{-1} was applied for two weeks with a 24 h stagnation period after 4 d. After two weeks, the flow velocity was increased to 1.7 m d^{-1} for 2 d to test the potential remobilizing effect of enhanced flow velocity on NP transport (Fig. 1b). To detect potential changes in environmental conditions, we continuously monitored EC (EC probe, TetraCon, WTW, Germany) in the column inflow (supernatant) and outflow as well as pH (SenTix 41, WTW) and redox potential (SenTix ORP, WTW, values were corrected for the standard potential of the redox probe relative to the hydrogen normal electrode at 20 °C, i.e. + 211 mV) in the column outflow (Fig. S4).

Effluent samples of the different depths for quantification of Ag were taken over the whole course of the experiment. Effluent samples for toxicity tests (1.5 L in 15, 30, and 90 cm depth) were taken during the expected breakthrough of highest NP concentrations (i.e. breakthrough of the tracer in the respective depth).. At the end of the experiment, columns were drained and subsequently, sediment samples were taken up to a depth of 75 cm using a soil auger (Pürckhauer, outer diameter 28 mm, inner diameter: 18 mm). Four sample cores were taken and separated into 2 cm intervals for the upper 30 cm, and into 5 cm intervals below. Additional samples of the topmost 10 cm, segmented into 1 cm intervals, were taken to measure organic carbon (C) and nitrogen (N) concentration in addition to Ag.

2.4. Laboratory column experiments

Clean sediment (termed as "pristine sediment") directly obtained from the manufacturer, and sediment aged in natural pond water (termed as "aged sediment") was used for the lab-scale column experiments. The optical difference between the columns was clearly visible: while the pristine sediment was a clean sediment, the aged sediments had layers of greenish-grey material on top as well as in different depths which were formed during column packing of the homogenized substrate under water-saturated conditions (Fig. 1d).

Like in outdoor experiments, the lab sediment columns were flushed with diluted pond water from the slow sand filtration pond. However, water was taken at a sampling point beneath the pond after passing a layer of filter sand. Therefore, natural colloids of the pond were mostly absent (i.e. remained in the sand layer) in the mobile phase of lab column experiments which led to low Fe concentrations, in contrast to the outdoor experiment (Table 1).

The column cylinders were made of polycarbonate with an inner diameter of 9.7 cm and 20 cm in height. The pristine columns were filled up to 15 cm with 1793 g sediment, resulting in a bulk density of 1.78 g cm^{-1}. The pond water-aged sediment was continuously saturated to preserve the physico-chemical and biological conditions of the system. The alteration of the natural, pond water-aged sediment (probably caused by accumulation of low density organic material and leaching of fines) led to a reduced bulk density of 1.4 g cm^{-3} (high flow) and 1.7 g cm^{-3} (low flow). Comparable to the outdoor experiment, a supernatant (4 mm) was adjusted, which ensured a continuous saturation of the column during the experiment. Both columns were enwrapped with aluminum foil to reduce the influence of light.

The columns were placed on a sintered glass plate embedded in a tripod, which sealed the column at the lower boundary. An irrigation device with 21 evenly distributed needles was installed on top of the columns to homogenously spread the suspension on the entire surface. A constant inflow of the different suspensions

was provided by a peristaltic pump. A flow rate of j = 0.2 and 0.7 m d^{-1}, respectively, was applied by a second peristaltic pump connected to the lower boundary (Fig. 1c). By using the same flow rate for both pumps, a stable flow field was adjusted (inflow = outflow). The effluent was continuously sampled by a fraction collector in 7.5 mL test tubes. To control the flow rates, both the suspension reservoir and the column setup were mounted on a balance and the masses were automatically recorded every 60 s.

All transport experiments were conducted in the same order: At first, a stable flow field was established by applying 3 pore volumes (PV) background solution (DI water for pristine columns, and diluted pond water for aged columns); followed by a tracer experiment with KBr (3 PV, EC = 820 μS cm^{-1}) and flushing of the column with 7 PV diluted pond water. The following NP-transport experiment was separated into 5 PV of Ag NP suspension application and flushing with 8 PV of diluted pond water.

Samples of the inflow NP suspension were taken to analyze NP concentrations and characterize physico-chemical parameters of the suspension (Table 1). At the end of the experiments, the entire sediment of each column was taken in 1 or 2 cm intervals except for the uppermost layer which was split into 2 samples: 0 to 0.2 cm and 0.2 to 1.0 cm.

2.5. Analyses

2.5.1. Particle size and ζ-potential

The colloidal stability of Ag NP used in lab column experiments was tested by time-resolved dynamic light scattering (DLS) measurements with a Zetasizer Nano ZS (Malvern Instruments). Silver NP were freshly mixed with diluted pond water including NOM and Ag@Au NP concentrations according to the experimental setup. The size of NP was measured for 24 h every 30 s. The highest peak of the size distribution (i.e. intensity-weighted Peak 1) was used for discussion of the data. The ζ-potential was measured before and after size measurement (Zetasizer Nano ZS, Malvern Instruments) and was calculated from electrophoretic mobility based on the Smoluchowsky approximation.

Particle properties in the supernatant of the outdoor experiment were analyzed by hydrodynamic chromatography (HDC) coupled to ICP-MS as the presence of natural colloids would interfere with DLS measurements. By HDC-ICP-MS, particles were separated by size via a HDC column and the isotopes ^{107}Ag, ^{109}Ag, ^{197}Au, and ^{27}Al were measured using ICP-MS. The retention time was used to estimate the NP size using citrate-stabilized gold NP (characterized by Rakcheev et al., 2013) as calibration standards, while the isotope composition allows NP identification. The size distributions were determined after signal deconvolution (see supporting information for more details).

The measurement procedure is described in detail by Degenkolb et al. (2018). Briefly, size separation was achieved at room temperature using PL-PSDA type 2 HDC column (separation range: 20–1200 nm. Agilent. Germany) connected to an HPLC system (Agilent 1220. Germany). The flow rate of the eluent (MQ water containing 1.8 mM sodium dodecyl sulphate, 3.2 mM Brij L23, 3.2 mM Triton X-100 and 7.46 mg L^{-1} D-penicillamine, adjusted to pH 10) was 2.1 mL min^{-1} and injection volume was 60 μL for samples and 5 μL for the internal standard. As internal standard for intensity drift correction and time marking, citrate-stabilized gold nanoparticles with a diameter of 5 nm (Sigma Aldrich) were used.

2.5.2. Quantification of silver in effluent and sediment samples

At the column outflow samples were taken for quantification of Ag concentrations as well as dissolved Ag breakthrough. Samples for NP quantification were stored in glass vessels at 4 °C in the dark until digestion and analysis. For quantification of dissolved Ag, samples were separated by centrifugal ultrafiltration (cut-off 50 kDa, Amicon Ultra-15 centrifugal filter device, Merck Millipore) directly after sampling and afterwards stored in plastic vessels at 4 °C in the dark until measurement by ICP-MS.

Aqueous samples were digested in HCl/HNO_3 (1:1 *v*/v) for Ag analysis using a two-step temperature program in the microwave (temperature ramp of 30 min from room temperature to 95 °C and subsequent 30 min irradiation at a constant temperature of 95 °C at 800 W). A volume of 10 mL sample was mixed with 4 mL of the acid mixture (final acid concentration of 4.5 and 9% for HCl and HNO_3, respectively) and digested in the microwave in Teflon tubes. Afterwards, samples were diluted to an acid concentration of 1.5% HCl and 3% HNO_3 with DI water.

All sediment samples were dried at 105 °C and homogenized in a disc vibrating mill (Retsch PM 40). For analysis of C and N a subsample of 20 g of the sediment was further ground to finer grain sizes (Narva Vibrator, GDR) and analyzed for total C and N (vario EL III, Elementar Analysensysteme). To calculate the amount of organic C, sediment samples were additionally dried at 600 °C and subsequently measured by CNS analyzer.

Sediment samples were digested in aqua regia as previous tests showed a good recovery for this method (data not shown). Here, 0.5 g sediment was weighed into microwave tubes and 5 mL of acid were added. A similar temperature program as for aqueous samples was applied. A centrifugation step (4.500 rpm, 30 min, Sorvall Lynx 6000, Thermo Scientific) followed the microwave digestion to remove undissolved solids. Silver concentrations were measured by ICP-MS (iCAP Q, Thermo Scientific).

Both methods as well as recovery rates are described by Metreveli et al. (in prep) in more detail.

2.6. Ecotoxicological tests

2.6.1. Test organism

Daphnia magna (Eurofins-GAB, Germany) were cultured in a climate-controlled chamber (Weiss Environmental Technology Inc., Germany) at 20 ± 1 °C applying a 16:8 h (light:dark) photoperiod (visible light intensity: 3.14 W/m^2; UVA: 0.01 W/m^2; UVB: 0.01 W/m^2; as detailed in Dabrunz et al., 2011). In groups of 25 individuals (age > 14 d), adult organisms were kept in 1.5 L of reconstituted hard freshwater recommended by ASTM International Standard Guide E729 (ASTM 2007). Additionally, the medium was enriched with selenium, vitamins (thiamine hydrochloride, cyanocobalamin, and biotin; ASTM-Medium), and seaweed extract (8.00 mg TOC L^{-1}; Marinure®, Glenside, Scotland). The culture medium was renewed three times a week and the animals were daily fed on *Desmodesmus* sp. (200 μg C per organism).

2.6.2. Toxicity studies

For each effluent of the different sampling depths (15, 30, and 90 cm) individual acute toxicity studies were carried out using *D. magna* as test organism. Moreover, the acute toxicity of the applied NP suspensions (^{109}Ag NP, and Ag@Au NP) was assessed individually and in mixture similar to the supernatant of the large-scale experiment (diluted pond water, 0.5 mg L^{-1} ^{109}Ag NP, 0.8 mg L^{-1} SR-NOM, and 0.6 mg L^{-1} Ag@Au NP). The conducted experiments were generally based on the OECD guideline 202 (OECD 2004), with a prolonged test duration to 96 h, as recommended for testing nanoparticulate substances (Dabrunz et al., 2011).

Five juvenile daphnids (age < 24 h) were exposed to increasing concentrations of the respective NP suspension (^{109}Ag NP: 0, 30, 40, 50, 60, 70, 80, and 100%; Ag@Au NP: 0, 33, 44, 56, 67, 78, 89, and 100%; Mix: 0, 0.25, 5, 10, 20, and 30% of the input concentration) and different column effluents (2.5, 5, 10, 20, 30, 50, and 100% of effluent from 15, 30, and 90 cm depth) using ASTM-Medium as test medium. Each applied concentration was repli-

cated four times. Every 24 h, daphnids were visually checked for their mobility. Animals were considered as immobile when the test beaker was gently agitated and no movement was recognizable within 10 s. Mobility data were used for the calculation of half maximal effect concentrations (EC_{50}), illustrating the concentration of NP suspension/column effluent causing immobility in 50% of the exposed daphnids.

2.7. Scanning electron microscopy

Scanning electron microscopy was used to visualize retained NP and the presence of organisms in the upper 1 cm of outdoor column sediments. Approximately 1 mg of sediment sample of each outdoor sediment column was air-dried on a silicon waver. Analyses were conducted at the Center for Electron Microscopy (ZELMI) of the TU Berlin with an low vacuum-SEM (GeminiSEM500 NanoVP, Zeiss) coupled with an EDX detector (Bruker Quantax XFlash 6I60; EDAX, software 'TEAM', detector 'Apollo' — acquisition parameters of the beam: accelerating voltage: 15 kV, chamber pressure: 84 Pa). Per sample, at least 20 different points were investigated under the microscope to get an impression of the distribution of Ag NP on the sediment.

3. Results

3.1. Nanoparticle properties

The absolute value of the ζ-potential of citrate stabilized Ag NP (originally −41.3 mV) was only slightly changed by SR-NOM coating (−38.6 mV) but was reduced in diluted pond water to −12 ± 1 mV. However, only slight aggregation was observed during 24 h of time-resolved DLS measurement: From an original size of 48 nm Ag NP size increased to a final diameter of 62 ± 12 nm (Polydispersity index (PdI) 0.3 ± 0.2) in the high flow experiment. During low flow experiment NP size changed from 66 ± 6 nm up to a size of 111 ± 12 nm (PdI 0.4 ± 0.0). In the high flow experiment, only ^{109}Ag NP with a background SR-NOM concentration of 0.8 ppm were applied. In the low flow experiment, Ag@Au NP were additionally present in the mixture, so that the size measured by DLS is an average of both kinds of NP. This explains the different results of DLS measurements for the low and high flow experiment.

A slight aggregation of NP was also observed in outdoor experiments by HDC-ICP-MS measurements (Fig. S5): ^{109}Ag NP with an initial particle size of 52.8 ± 2.3 nm aggregated to diameters of 101.8 ± 8.9 nm. Despite of the presence of natural colloids in the outdoor columns, the observed aggregates seemed to be Ag NP homoaggregates as their size was exactly twice as large as primary particles. Sizes measured by HDC-ICP-MS suggest that heteroaggregation with Ag@Au NP was not predominant but may have occurred sporadically.

3.2. Comparison of pristine and aged sediment column properties

Sediments of all column experiments were analyzed for total C and N concentration. Due to seasonal changes in the ecological community in pond water and on sediments, values differed between the aged sediments of the three different column experiments (Figs. 2a, S6). Additionally, columns of the outdoor experiment represent an undisturbed sediment profile, whereas lab columns were filled with homogenized sediment material.

Generally, aged sediments had higher N concentrations than pristine sediments (0.02 ± 0.01% in aged sediments compared to 0.003 ± 0.000% in pristine sediments, Fig. 2a). Outdoor columns and low flow lab columns showed higher N concentrations in the upper sediment layers. High flow lab columns had highest N concentrations of all sediments without a gradient in depth.

Organic carbon concentrations fluctuated strongly and were generally very low, but except for the high flow experiment did not differ between aged and pristine sediments (0.27 ± 0.21% in aged sediments compared to 0.13 ± 0.05 in pristine sediments, Fig. S6). The C/N ratio tended to be lower in aged sediments, but trends were not clear (20.5 ± 9.0% in aged sediments compared to 39.5 ± 15.6% in pristine sediments, Fig. S6).

Electron microscopy showed the presence of diatoms in the first centimeter of the outdoor columns (Fig. 2b). Additionally, cyanobacteria, green algae, and nematodes were identified under the light microscope in the first centimeter of sediments from lab as well as outdoor experiments (Fig. S7).

3.3. Outdoor column experiment

In the column supernatant, total ^{109}Ag concentrations of 533 ± 180 μg L^{-1} were detected; <0.5% was dissolved Ag^+ (0.05–

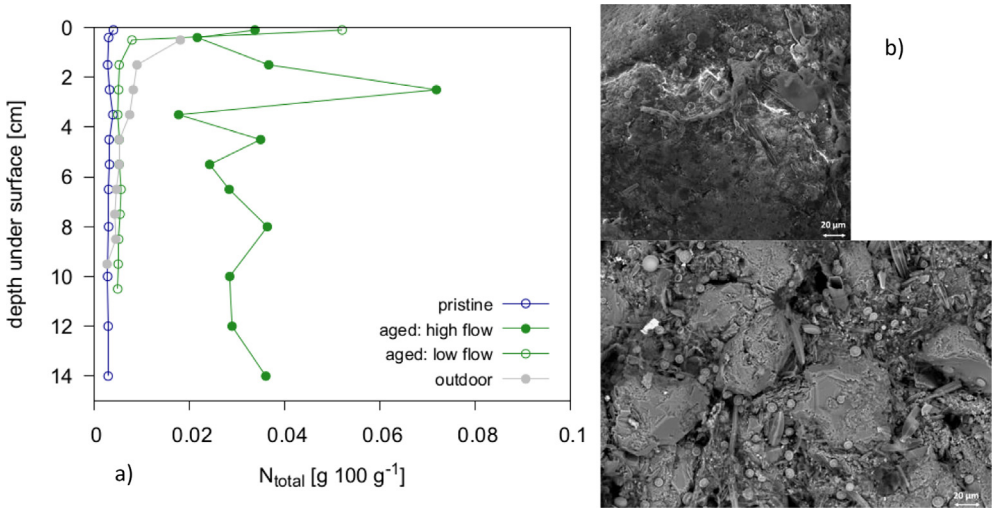

Fig. 2. a) N concentration in pond water-aged sediments of outdoor (grey) and lab (green) column experiments at high (filled circles) and low (open circles) flow conditions in comparison to pristine (blue) sediments; b) Diatoms in the upper centimeter of the sediment of outdoor experiments, visualized by SEM (lower image: back-scattered electron detector, upper image: variable pressure secondary electron detector, both: voltage 15 kV, pressure 84 Pa). (For interpretation of the references to colour in this figure legend, the reader is referred to the web version of this article.)

1.6 μg L). Silver NP breakthrough was observed as single and rare events in the uppermost depth of 15 cm (Fig. 3); below, no NP breakthrough occurred. Silver concentrations during the single breakthrough events were very low (between 0.1 μg L^{-1} and 1.6 μg L^{-1}) and mainly occurred during the first 5 PV, i.e. during NP application (phase I), or directly after changing to diluted pond water application (phase II). The stagnation period (phase III) and the high flow scenario (phase V) did not show any effect on NP breakthrough.

High ^{109}Ag contents in the sediments of both columns were observed after one month of flushing with diluted pond water for the top 25 cm of the columns. The Ag NP content was decreasing with depth illustrating high accumulation in the upper 10 cm of the columns (Fig. 4 for 0–30 cm and Fig. S8 for 0–75 cm). The indicated error bars from different sampling locations display the high local variability of Ag contents in the column sediment. However, the shape of the profile was detected for both columns, and is in line with the findings of the outdoor low flow experiment of Degenkolb et al. (2018) as illustrated in Fig. 4.

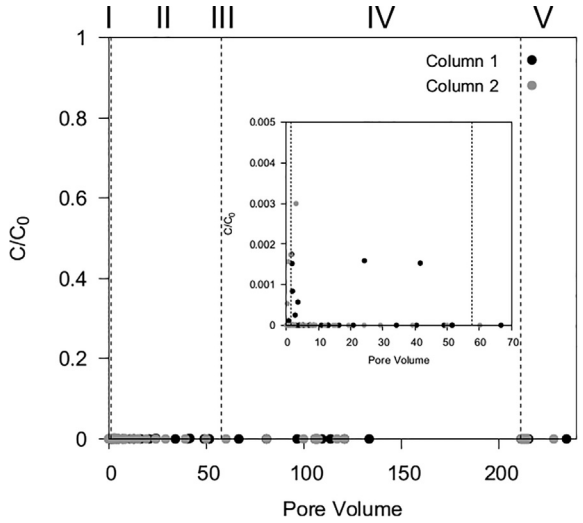

Fig. 3. Erratic breakthrough events in a sampling depth of 15 cm in outdoor experiments for the two replicate columns (grey and black circles). Roman numerals mark the phases of the experiment: I) NP application, II) diluted pond water application at flow rate of 0.7 m d^{-1}, III) stagnation, IV) diluted pond water application at flow rate of 0.7 m d^{-1}, and V) diluted pond water application at flow rate of 1.7 m d^{-1}.

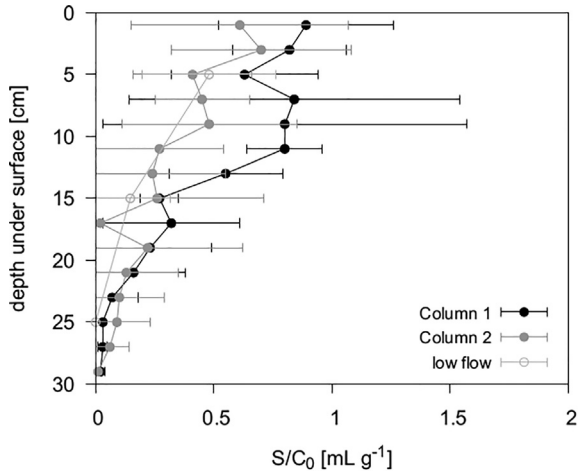

Fig. 4. ^{109}Ag retention profile for the upper 30 cm of sediments for both columns. The error bars margin the 95% confidence interval by two times standard error of 3–4 replicates. For comparison, values gained by Degenkolb et al. (2018) are included as low flow scenario.

3.4. Ecotoxicity tests

The 96- h EC_{50} values were evaluated to test the ecotoxicity of Ag NP-containing suspensions entering the riverbank filtration system. In addition, the toxicity of the single particle suspensions (i.e. ^{109}Ag NP and Ag@Au NP) was investigated. The lowest EC_{50} was observed for the mixture (~0.09 mg L^{-1}), followed by ^{109}Ag NP (~0.14 mg L^{-1}), and Ag@Au NP (~0.19 mg L^{-1}; Fig. S9 and Table S 1). In contrast, none of the applied effluent suspensions caused any immobility in the test organisms due to the extremely low or absent Ag NP breakthrough in all depths.

3.5. Lab column experiments

The analysis of the tracer experiments is in good agreement with the gained pore water velocities of the outdoor and laboratory experiments for both flow rates (Fig. S10). Only diffusion was higher in the aged sediment column at high flow rate compared to the outdoor experiment and the pristine sediment column.

The input Ag NP suspensions of low and high flow lab experiments had a ^{109}Ag concentration of 559 ± 133 and 691 ± 327 μg L^{-1}, respectively, with a dissolved Ag^+ concentration between 0.5 and 6.9 μg L^{-1}.

In pristine sediment columns, almost no NP were measured in outflow samples, but some erratic peaks occurred (Fig. 5). For the low flow scenario, low concentrations of <0.5% of initial NP concentration were measured after 1 PV. For the high flow experiment, no Ag NP breakthrough was observed. Both during high flow and low flow experiments, a single point of Ag breakthrough occurred after changing the inflow from NP suspension to flushing solution (i.e. diluted pond water without Ag NP) which seemed to mobilize a part of retained Ag NP.

In accordance with the breakthrough results, we found large Ag NP contents in the upper part (0–7 cm) of both columns after the end of the experiments (Fig. 6). When sediments were aged in pond water with accumulation of organic materials, no Ag NP breakthrough was observed for neither low nor high flow rates

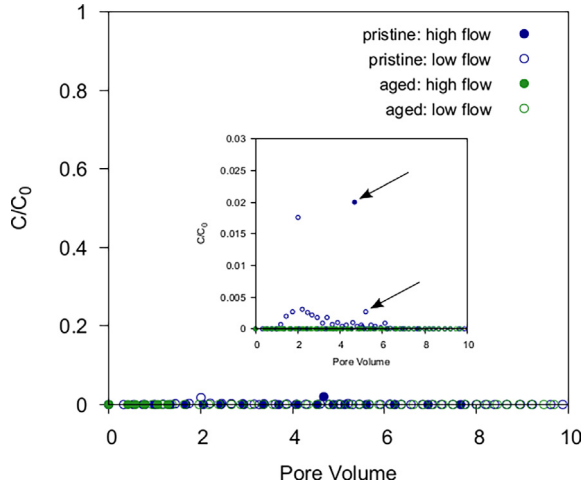

Fig. 5. Breakthrough of Ag NP in lab column experiments for both pristine (blue) and aged (green) sediment at high (filled circles) and low (open circles) flow rates: single release events of Ag NP took place in pristine columns. Arrows mark the samples taken after changing from NP suspension to diluted pond water. (For interpretation of the references to colour in this figure legend, the reader is referred to the web version of this article.)

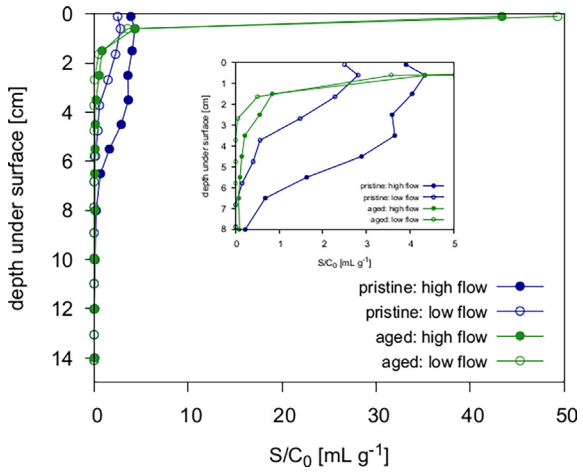

Fig. 6. ^{109}Ag NP retention profiles in pristine (blue) and aged (green) sediments under high flow (filled circles) and low flow (open circles) rate. (For interpretation of the references to colour in this figure legend, the reader is referred to the web version of this article.)

(Fig. 5). In contrast to the retention in pristine sediments, Ag NP were accumulated at the very top of the columns and transported not further than 2 cm, irrespective of flow velocity (Fig. 6).

3.6. Mass balance of column experiments

Almost all Ag NP applied in our column experiments were retained in the column sediments with a recovery of 102 ± 32%. However, this retention had a high spatial variability (Table 2), especially in the outdoor experiments. In lab experiments, the complete sediment was dried and homogenized by milling, but only 0.5 g of sediment of each depth was analyzed. Furthermore, highest Ag concentrations at the top of the columns made the mass balance very sensitive to the estimated thickness and bulk density of the upper layers. For the pristine lab experiments, the Ag recovery was significantly lower for the low flow experiment (58.8%) compared to the high flow experiment (140.8%).

4. Discussion

4.1. The presence of biological components in aged sediments

Both outdoor and aged lab column sediments contained high concentrations of N, especially in the upper centimeters (Fig. 2a). We presume that this is caused by the activity of N-fixing cyanobacteria that are dependent on light available on the surface of the columns. Highest N concentrations distributed over the complete column (high flow scenario) were measured in sediments taken in late autumn (November 2018), when cyanobacteria were not active anymore (Caron et al., 1985). Dead organic material settled on the sediments of the column in large amounts and decomposers' activity was already reduced so that biological substances accumulated on top of the columns (Buscail et al., 1995). This is also supported by the high organic C concentrations in the sediments of the high flow lab experiment as C was distributed over the entire sediment profile during sediment sampling and homogenization for the lab experiments. The high amount of organic material in the high flow experiment can be one explanation of the lower bulk density (1.4 g cm^3 compared to 1.7 g cm^3) of the sediments as well as the stronger effect of diffusion on tracer breakthrough displayed in Fig. S10.

The presence of living organisms in the upper centimeter of aged lab and outdoor columns was proven by electron and light microscopy. A high number of diatoms (Fig. 2b) as well as cyanobacteria, green algae, and nematodes (Fig. S7) confirm that aged sediments exhibited a high biological activity.

4.2. Nanoparticle reactions in the column system

Before addition to the columns, citrate-stabilized Ag NP were coated by SR-NOM to enhance the comparability with NP possibly present in natural systems. While the surface charge of citrate stabilized Ag NP is negative both in the presence and absence of SR-NOM, NOM enhances steric repulsion between NP and sediment surfaces which enhances NP stability. Still, Ag NP surface charge was reduced in diluted pond water with Ca^{2+} concentrations of 0.7 mM and Ag NP aggregated slightly. Divalent cations and especially Ca^{2+} are well-known to cause NP aggregation by bridging between organically coated NP and charge neutralization by compression of the electrical double layer of NP (Philippe and Schaumann, 2014). However, the measured particle sizes in high and low flow experiments of 62 and 111 nm, respectively, are much smaller than the pores of the sediment columns where approximately 75% of the water is stored in pores with a radius larger than 1 μm (according to water content and grain size distribution). Therefore, the slight aggregation will not cause significant mechanical filtration and NP-to grain size- ratio is too small to expect any straining effects or surface filtration (Bradford et al., 2006; McDowell-Boyer et al., 1986).

As observed by the use of ultracentrifugation, only samples of the column supernatant contained dissolved Ag^+ ions. In the effluent, no Ag^+ was observed. This suggests that Ag NP dissolution was no relevant process during the column experiment. However, potentially existing Ag^+ ions might also have sorbed to the solid phase of the porous system.

4.3. Effect of flow velocity on NP transport and retention

The transport experiments in lab columns with pristine sediments seem to support our expectation that increasing flow rates would enhance NP transport as retention profiles showed Ag NP transport into greater depths when flow velocities were higher. However, due to the significant differences in mass recovery (Table 2) and the resulting uncertainties of the absolute measured concentrations this hypothesis can neither be confirmed nor denied definitely. By analyzing the shape of the profiles, the respective maximum retention of Ag NP was measured in a depth of 2 cm for the low flow scenario and 4 cm for the high flow scenario. Below, Ag concentrations in the sediment sharply decrease in both experiments.

In lab experiments with aged sediments as well as in outdoor experiments no differences were observed in transport and retention under different flow rates. In the lab columns, no NP break-

Table 2
Recovery of Ag in sediments of column experiments.

Lab experiments				Outdoor experiments	
Pristine, low	Pristine, high	Aged, low	Aged, high	Column 1	Column 2
58.7%	140.8%	98.2%	77.4%	178 ± 63%	95 ± 16%

through was determined under aged conditions and NP were accumulated in the uppermost 2 mm of the column with no transport below 2 cm depth, irrespective of flow velocity. This suggests that diffusion to attachment sites does not limit NP retention in aged sediments as increasing flow rate does not lead to enhanced NP transport in case of the presence of biological components. Also in near-natural outdoor columns results at 0.7 m d^{-1} flow velocity are comparable to findings at lower flow rate (0.2 m d^{-1}, published by Degenkolb et al., 2018). Hence, even 3.5-fold higher flow rates do not lead to NP transport in aged, biomass-containing saturated sediments, such as riverbank filtration systems.

In general, NP mobility was low under all tested conditions in our study. Both flow conditions used in our column experiments (i.e. 0.2 and 0.7 m d^{-1}) are in the range of natural flow velocities in sandy aquifers (Kunkel and Wendland, 1997) and smaller than most flow velocities applied in previous studies. Therefore, NP mass transfer in our study is strongly affected by diffusion to and sorption on the solid phase instead of advection which leads to high NP deposition (Braun et al., 2015). In combination with the low NP concentration (0.6 mg L^{-1} in our study compared to 3–45 mg L^{-1} in other studies), this explains the lack of NP breakthrough which is in contrast to a variety of other studies using citrate coated Ag NP in comparable porous media (El Badawy et al., 2013; Li et al., 2013; Taghavy et al., 2013). These authors used flow rates between 15 and 55 m d^{-1} which is 20–80 times larger than the high flow rate used in our study. A decreased residence time of NP in the pore space due to higher flow rates can reduce the possibility for NP to interact with potential attachment sites. Additionally, a reduced flow rate has been shown to enhance the possibility for NP diffusion in small pore spaces and to increase attachment efficiency in diffusion-determined colloid systems as soon as hydrodynamic drag forces of the water flow overcome interaction forces of colloids with sediment surfaces (Chang and Chan, 2008).

Moreover, a stronger Ag NP stabilization by organic coatings and very high NP concentrations (i.e. 60 mg L^{-1}) can cause Ag NP breakthrough even at flow velocities as low as 0.05 m d^{-1} (Braun et al., 2015). This illustrates that although flow velocity is of high importance for NP mobility, factors such as colloidal stability and NP concentration also affect NP transport. Nevertheless, environmental concentrations of engineered NP are currently in the ng-μg L^{-1} range (Gottschalk et al., 2009) and industrial coatings may be replaced or covered by less stabilizing natural coating agents (Louie et al., 2016), which highlights the environmental relevance of the results of our experiments.

4.4. The role of biomass for NP retention

The presence of biomass in lab column experiments prevented any breakthrough of Ag NP. While a small breakthrough curve (<0.5% of initially injected NP) at low flow velocity, and single, erratic breakthrough events with higher Ag concentrations at high and low flow velocity were observed for pristine sediments, no Ag was detected in the outflow of aged sediment columns. Furthermore, NP deposition on biological surfaces was unaffected by increasing flow velocity.

Under abiotic conditions, attachment is expected to mainly occur on oppositely charged metal oxides and clay minerals as well as by Ca^{2+}-NOM bridging between coated NP and sediment surfaces. As sediment material contained trace amounts of several elements such as Fe, Al, and Ti, physico-chemical filtration on these surfaces seems to occur in pristine sediment columns. The determined maximum retention of Ag NP in the lab experiments with pristine sediment was between 1.3 and 1.6 μg/g for the low flow scenario and 2.4 to 3.0 μg/g for the high flow scenario in the first centimeters. Hence, the abiotic sediment provides geogenic attachment sites for negatively charged Ag NP. However, the progress of the retention front down to a depth of 2–4 cm and the erratic breakthrough of NP shows that these geogenic attachment sites are limited.

In contrast, the occurrence of biological components highly increased the maximum retention capacity of the material up to 27.6 μg/g in the low flow and 30.0 μg/g in the high flow column experiment. Enhanced deposition of Ag NP in aged sediments can be related to mechanical filtration and straining as organic matter reduces the pore space of the sediment (Bradford et al., 2011). Additionally, aged sediment surfaces may offer a higher surface roughness than pristine sediments which might have increased NP-sediment interactions (Hoek et al., 2003). However, mechanical retention is not likely in our sediment system due to the large NP-grain size ratio. More importantly, biological surfaces offer a large number of versatile attachment sites for Ag NP so that NP are retained in the sediment system by chemical interactions. The presence of biocolloids such as proteins, bacteria, and polysaccharides offer various possibilities for interaction with NP. Covalent bonds to functional groups of organic matter are expected to lead to high interaction forces between biological components and Ag NP (Avellan et al., 2018; Nevius et al., 2012). Therefore, NP retention in aged sediments is high and NP are retained in the uppermost layers of the sediment.

In spite of the presence of biomass in outdoor columns, single, erratic breakthrough events were detected in the near-natural system, both at low and high flow velocity. This transport behavior is more comparable to the breakthrough in pristine lab columns, although sediment properties resemble the aged lab columns. Furthermore, Ag NP are transported in depths up to 25 cm in the outdoor column, but were retained on the column surface of aged sediments in the lab. These differences might be the result of the longer duration of the outdoor experiments, leading to slow NP transport through the outdoor sediment system. Potentially, degradation of organic matter in the sediment columns may be one reason for NP detachment and transport at longer experiment duration. Additionally, it has to be noted that sampling by the soil auger may have led to NP carryover in deeper sediment layers so that the transport depth might be overestimated in outdoor experiments.

The erratic breakthrough events, both observed in pristine lab experiments and outdoor columns illustrate that retained NP may be remobilizable under certain circumstances. However, the responsible processes are not well-understood, yet. As the remobilization was also observed in pristine sediment columns it might be an abiotic mechanism. For example, NP interactions with the solid-water interface may not be strong enough so that small changes in environmental conditions remobilize a part of NP which breaks through at the column outflow. This assumption is supported by the observation in lab columns that breakthrough of Ag NP occurred when changing the input suspension from NP-containing pond water to NP-free pond water.

4.5. Nanoparticles in surface waters- a risk for potential drinking water resources?

Both lab and outdoor experiments clearly showed a very low Ag NP mobility in riverbank filtration systems at flow velocities between 0.2 and 0.7 m d^{-1} and NP concentrations of 0.6 mg L^{-1}. Sediment surfaces and biomass offer a variety of attachment sites for NP and low flow rates enable the diffusion to and interaction with these sites. An aged sediment system with a well-established flora and fauna has a higher retention capacity for Ag NP than pristine sediments. Even the enhancement of flow velocity to 1.7 m d^{-1}, did not cause significant remobilization of retained Ag NP. However, previous batch experiments suggest a remobilization

potential for Ag NP retained in aged sediments of the riverbank filtration system (Degenkolb et al., 2018). Probably, the 2.4-fold higher flow velocity during the high flow scenario in the outdoor experiment caused much lower shear forces than tested in the batch experiments of Degenkolb et al. (2018). Moreover, hydrochemical conditions remained constant during the high flow rate. During increasing flow rates in natural systems which may be caused by heavy rain events, water chemistry is expected to change which was shown to be effective in remobilizing NP when combined with mechanical forces (Degenkolb et al., 2018; Metreveli et al., 2015).

The almost complete retention of NP on the solid phase of the porous system led to an efficient detoxification of NP-containing suspensions. The high toxicity of NP input suspension to *Daphnia magna* was completely eliminated after passage through 15 cm of a near-natural riverbank filtration system. This suggests a high potential of riverbank filtration for cleaning NP-containing surface water.

5. Conclusions

Overall, our experiments point out, that retention mechanisms of NP in saturated sediments are highly affected by the presence of biomass. Naturally occurring aging processes on riverbank filtration sediments enhance the efficiency of the system to retain potential NP contaminations in surface water. When biological material is present, NP immediately undergo attachment and deposition and accumulate in the uppermost sediment layers. This may explain the consistent observation of NP fate studies finding NP accumulation mainly in surficial sediment layers of aquatic ecosystems (Espinasse et al., 2018; Geitner et al., 2018; Lowry et al., 2012). Our results suggest that even at increasing flow rates NP attachment on biological material is efficient. However, NP breakthrough can occur in erratic, single peaks, a process that is not well-understood, yet, and needs future research. At larger time scales and in more complex systems, NP transport in deeper sediment layers may therefore take place.

Abiotic retention mechanisms (i.e. interaction with iron oxides, clay minerals or bridging processes in the presence of multivalent cations) also offer great potential for NP retention. Still, these mechanisms allow NP transport in deeper sediment layers. Although our results suggest that the risk for NP transport in riverbank filtrates is low, a constant NP input may lead to ecotoxicological relevant NP concentrations in upper sediments. Especially in areas of waste water discharge, constant NP introduction in surface water and deposition on sediments can be expected. Grazing organisms will feed on those contaminated sediments which might even lead to Ag NP accumulation in the food chain.

Declaration of Competing Interest

The authors declare that there is no conflict of interest regarding the publication of this article.

Acknowledgements

Many people were involved helping in the outdoor and lab experiments. We especially want to thank Silke Pabst, Eduard Sandyk, and Perry Maroz for their dedicated help in the outdoor column experiments and sample preparation in the lab. For measurements at the ICP-MS we thank Claudia Kuntz (TU Berlin) and Hans-Joachim Stärk (UFZ Halle-Leipzig). For the cooperation and help with Au measurements we thank Alexander Kämpfe and Christoph Merdan from the German Environment Agency (UBA). Furthermore, we want to thank Sabine Rautenberg for sample preparation and CNS measurements and Christoph Fahrenson (ZELMI, TU Berlin) for the support during SEM analysis.

The authors acknowledge financial support by the German Research Foundation (DFG) within the research unit FOR 1536 INTERNANO and its subprojects KA 1139/18-2, KL 2909/2, SCHU 2271/5-2, BA 1592/6-2 and VO 566/12-2.

Appendix A. Supplementary data

Supplementary data to this article can be found online at https://doi.org/10.1016/j.scitotenv.2019.134387.

References

Adrian, Y.F., Schneidewind, U., Bradford, S.A., Simunek, J., Fernandez-Steeger, T.M., Azzam, R., 2018. Transport and retention of surfactant- and polymer-stabilized engineered silver nanoparticles in silicate-dominated aquifer material. Environ. Pollut. 236, 195–207. https://doi.org/10.1016/j.envpol.2018.01.011.

Andreï, J., Pain-Devin, S., Felten, V., Devin, S., Giambérini, L., Mehennaoui, K., Cambier, S., Gutleb, A.C., Guérold, F., 2016. Silver nanoparticles impact the functional role of Gammarus roeseli (Crustacea Amphipoda). Environ. Pollut. 208, 608–618. https://doi.org/10.1016/j.envpol.2015.10.036.

Avellan, A., Simonin, M., McGivney, E., Bossa, N., Spielman-Sun, E., Rocca, J.D., Bernhardt, E.S., Geitner, N.K., Unrine, J.M., Wiesner, M.R., Lowry, G.V., 2018. Gold nanoparticle biodissolution by a freshwater macrophyte and its associated microbiome. Nat. Nanotechnol. 1. https://doi.org/10.1038/s41565-018-0231-y.

Ben-Moshe, T., Dror, I., Berkowitz, B., 2010. Transport of metal oxide nanoparticles in saturated porous media. Chemosphere 81, 387–393. https://doi.org/10.1016/j.chemosphere.2010.07.007.

Bradford, S.A., Simunek, J., Bettahar, M., van Genuchten, M.T., Yates, S.R., 2006. Significance of straining in colloid deposition: evidence and implications: SIGNIFICANCE OF STRAINING IN COLLOID DEPOSITION. Water Resour. Res. 42. https://doi.org/10.1029/2005WR004791.

Bradford, S.A., Torkzaban, S., Simunek, J., 2011. Modeling colloid transport and retention in saturated porous media under unfavorable attachment conditions: MODELING COLLOID TRANSPORT AND RETENTION. Water Resour. Res. 47. https://doi.org/10.1029/2011WR010812.

Braun, A., Klumpp, E., Azzam, R., Neukum, C., 2015. Transport and deposition of stabilized engineered silver nanoparticles in water saturated loamy sand and silty loam. Science of The Total Environment, Special Issue: Engineered nanoparticles in soils and waters 535, 102–112. https://doi.org/10.1016/j.scitotenv.2014.12.023.

Buscail, R., Pocklington, R., Germain, C., 1995. Seasonal variability of the organic matter in a sedimentary coastal environment: sources, degradation and accumulation (continental shelf of the Gulf of Lions—northwestern Mediterranean Sea). Cont. Shelf Res. 15, 843–869. https://doi.org/10.1016/0278-4343(94)E0035-K.

Caron, D.A., Pick, F.R., Lean, D.R.S., 1985. Chroococcoid cyanobacteria in Lake Ontario: vertical and seasonal distributions during 1982. J. Phycol. 21, 171–175. https://doi.org/10.1111/j.0022-3646.1985.00171.x.

Chang, Y.-I., Chan, H.-C., 2008. Correlation equation for predicting filter coefficient under unfavorable deposition conditions. AICHE J. 54, 1235–1253. https://doi.org/10.1002/aic.11466.

Chen, G., Liu, X., Su, C., 2012. Distinct effects of humic acid on transport and retention of TiO_2 rutile nanoparticles in saturated sand columns. Environ. Sci. Technol. 46, 7142–7150. https://doi.org/10.1021/es204010g.

Cornelis, G., Pang, L., Doolette, C., Kirby, J.K., McLaughlin, M.J., 2013. Transport of silver nanoparticles in saturated columns of natural soils. Sci. Total Environ. 463–464, 120–130. https://doi.org/10.1016/j.scitotenv.2013.05.089.

Dabrunz, A., Duester, L., Prasse, C., Seitz, F., Rosenfeldt, R., Schilde, C., Schaumann, G. E., Schulz, R., 2011. Biological surface coating and molting inhibition as mechanisms of TiO2 nanoparticle toxicity in Daphnia magna. PLoS One 6,. https://doi.org/10.1371/journal.pone.0020112 e20112.

Degenkolb, L., Metreveli, G., Philippe, A., Brandt, A., Leopold, K., Zehlike, L., Vogel, H.-J., Schaumann, G.E., Baumann, T., Kaupenjohann, M., Lang, F., Kumahor, S.K., Klitzke, S., 2018. Retention and remobilization mechanisms of environmentally aged silver nanoparticles in an artificial riverbank filtration system. Sci. Total Environ. 645, 192–204. https://doi.org/10.1016/j.scitotenv.2018.07.079 0048-9697.

Derjaguin, B., Landau, L., 1941. Theory of stability of highly charged lyophobic sols and adhesion of highly charged particles in solutions of electrolytes. Acta Physicochim. USSR, 633–662.

El Badawy, A.M., Aly Hassan, A., Scheckel, K.G., Suidan, M.T., Tolaymat, T.M., 2013. Key factors controlling the transport of silver nanoparticles in porous media. Environmental Science & Technology 47, 4039–4045. https://doi.org/10.1021/es304580r.

Espinasse, B.P., Geitner, N.K., Schierz, A., Therezien, M., Richardson, C.J., Lowry, G.V., Ferguson, L., Wiesner, M.R., 2018. Comparative persistence of engineered nanoparticles in a complex aquatic ecosystem. Environmental Science & Technology 52, 4072–4078. https://doi.org/10.1021/acs.est.7b06142.

Fabrega, J., Luoma, S.N., Tyler, C.R., Galloway, T.S., Lead, J.R., 2011. Silver nanoparticles: behaviour and effects in the aquatic environment. Environ. Int. 37, 517–531. https://doi.org/10.1016/j.envint.2010.10.012.

Geitner, N.K., Cooper, J.L., Avellan, A., Castellon, B.T., Perrotta, B.G., Bossa, N., Simonin, M., Anderson, S.M., Inoue, S., Hochella, M.F., Richardson, C.J., Bernhardt, E.S., Lowry, G.V., Ferguson, P.L., Matson, C.W., King, R.S., Unrine, J. M., Wiesner, M.R., Hsu-Kim, H., 2018. Size-based differential transport, uptake, and mass distribution of ceria (CeO_2) nanoparticles in wetland mesocosms. Environmental Science & Technology 52, 9768–9776. https://doi.org/10.1021/acs.est.8b02040.

Gottschalk, F., Sonderer, T., Scholz, R.W., Nowack, B., 2009. Modeled environmental concentrations of engineered nanomaterials (TiO_2, ZnO, ag, CNT, fullerenes) for different regions. Environ. Sci. Technol. 43, 9216–9222. https://doi.org/10.1021/es9015553.

Hoek, E.M.V., Bhattacharjee, S., Elimelech, M., 2003. Effect of membrane surface roughness on colloid–membrane DLVO interactions. Langmuir 19, 4836–4847. https://doi.org/10.1021/la027083c.

Hoffmann, A., Gunkel, G., 2011. Bank filtration in the sandy littoral zone of Lake Tegel (Berlin): structure and dynamics of the biological active filter zone and clogging processes. Limnologica 41, 10–19. https://doi.org/10.1016/j.limno.2009.12.003.

Klitzke, S., Metreveli, G., Peters, A., Schaumann, G.E., Lang, F., 2015. The fate of silver nanoparticles in soil solution — sorption of solutes and aggregation. Sci. Total Environ. 535, 54–60. https://doi.org/10.1016/j.scitotenv.2014.10.108.

Kumahor, S.K., Hron, P., Metreveli, G., Schaumann, G.E., Klitzke, S., Lang, F., Vogel, H.-J., 2016. Transport of soil-aged silver nanoparticles in unsaturated sand. J. Contam. Hydrol. 195, 31–39. https://doi.org/10.1016/j.jconhyd.2016.10.001.

Kunkel, R., Wendland, F., 1997. WEKU - a GIS-supported stochastic model of groundwater residence times in upper aquifers for the supraregional groundwater management. Environ. Geol. 30, 1–9. https://doi.org/10.1007/s002540050126.

Lecoanet, H.F., Wiesner, M.R., 2004. Velocity effects on fullerene and oxide nanoparticle deposition in porous media. Environ. Sci. Technol. 38, 4377–4382. https://doi.org/10.1021/es035354f.

Li, Q., Mahendra, S., Lyon, D.Y., Brunet, L., Liga, M.V., Li, D., Alvarez, P.J.J., 2008. Antimicrobial nanomaterials for water disinfection and microbial control: potential applications and implications. Water Res. 42, 4591–4602. https://doi.org/10.1016/j.watres.2008.08.015.

Li, Z., Aly Hassan, A., Sahle-Demessie, E., Sorial, G.A., 2013. Transport of nanoparticles with dispersant through biofilm coated drinking water sand filters. Water Res. 47, 6457–6466. https://doi.org/10.1016/j.watres.2013.08.026.

Lin, S., Cheng, Y., Bobcombe, Y., L Jones, K., Liu, J., Wiesner, M.R., 2011. Deposition of silver nanoparticles in geochemically heterogeneous porous media: predicting affinity from surface composition analysis. Environ. Sci. Technol. 45, 5209–5215. https://doi.org/10.1021/es2002327.

Louie, S.M., Tilton, R.D., Lowry, G.V., 2016. Critical review: impacts of macromolecular coatings on critical physicochemical processes controlling environmental fate of nanomaterials. Environmental Science: Nano 3, 283–310. https://doi.org/10.1039/C5EN00104H.

Lowry, G.V., Gregory, K.B., Apte, S.C., Lead, J.R., 2012. Transformations of nanomaterials in the environment. Environmental Science & Technology 46, 6893–6899. https://doi.org/10.1021/es300839e.

McDowell-Boyer, L.M., Hunt, J.R., Sitar, N., 1986. Particle transport through porous media. Water Resour. Res. 22, 1901–1921. https://doi.org/10.1029/WR022i013p01901.

Metreveli, G., Philippe, A., Schaumann, G.E., 2015. Disaggregation of silver nanoparticle homoaggregates in a river water matrix. Sci. Total Environ. 535, 35–44. https://doi.org/10.1016/j.scitotenv.2014.11.058.

Metreveli, G., David, J., Schneider, R., Kurtz, S., Degenkolb, L., Schaumann, G., 2019. Sulfidized and Isotopically Enriched Silver Nanoparticles for Long Term Mesocosm Studies: Preparation, Characterization, and Quantification (in prep.).

Nevius, B.A., Chen, Y.P., Ferry, J.L., Decho, A.W., 2012. Surface-functionalization effects on uptake of fluorescent polystyrene nanoparticles by model biofilms. Ecotoxicology 21, 2205–2213. https://doi.org/10.1007/s10646-012-0975-3.

Petosa, A.R., Öhl, C., Rajput, F., Tufenkji, N., 2013. Mobility of nanosized cerium dioxide and polymeric capsules in quartz and loamy sands saturated with model and natural groundwaters. Water Res. 47, 5889–5900. https://doi.org/10.1016/j.watres.2013.07.006.

Philippe, A., Schaumann, G.E., 2014. Interactions of dissolved organic matter with natural and engineered inorganic colloids: a review. Environmental Science & Technology 48, 8946–8962. https://doi.org/10.1021/es502342r.

Rajala, J.E., Vehniäinen, E.-R., Väisänen, A., Kukkonen, J.V.K., 2018. Toxicity of silver nanoparticles to Lumbriculus variegatus is a function of dissolved silver and promoted by low sediment pH. Environ. Toxicol. Chem. 37, 1889–1897. https://doi.org/10.1002/etc.4136.

Rakcheev, D., Philippe, A., Schaumann, G.E., 2013. Hydrodynamic chromatography coupled with single particle-inductively coupled plasma mass spectrometry for investigating nanoparticles agglomerates. Anal. Chem. 85, 10643–10647. https://doi.org/10.1021/ac4019395.

Ribeiro, F., Van Gestel, C.A.M., Pavlaki, M.D., Azevedo, S., Soares, A.M.V.M., Loureiro, S., 2017. Bioaccumulation of silver in Daphnia magna: waterborne and dietary exposure to nanoparticles and dissolved silver. Sci. Total Environ. 574, 1633–1639. https://doi.org/10.1016/j.scitotenv.2016.08.204.

Sagee, O., Dror, I., Berkowitz, B., 2012. Transport of silver nanoparticles (AgNPs) in soil. Chemosphere 88, 670–675. https://doi.org/10.1016/j.chemosphere.2012.03.055.

Sani-Kast, N., Labille, J., Ollivier, P., Slomberg, D., Hungerbühler, K., Scheringer, M., 2017. A network perspective reveals decreasing material diversity in studies on nanoparticle interactions with dissolved organic matter. Proc. Natl. Acad. Sci. 114, E1756–E1765. https://doi.org/10.1073/pnas.1608106114.

Schubert, J., 2002. Hydraulic aspects of riverbank filtration—field studies. J. Hydrol. 266, 145–161. https://doi.org/10.1016/S0022-1694(02)00159-2.

Sprenger, C., Hartog, N., Hernández, M., Vilanova, E., Grützmacher, G., Scheibler, F., Hannappel, S., 2017. Inventory of managed aquifer recharge sites in Europe: historical development, current situation and perspectives. Hydrogeol. J. 25, 1909–1922. https://doi.org/10.1007/s10040-017-1554-8.

Sun, P., Shijirbaatar, A., Fang, J., Owens, G., Lin, D., Zhang, K., 2015. Distinguishable transport behavior of zinc oxide nanoparticles in silica sand and soil columns. Sci. Total Environ. 505, 189–198. https://doi.org/10.1016/j.scitotenv.2014.09.095.

Taghavy, A., Mittelman, A., Wang, Y., Pennell, K.D., Abriola, L.M., 2013. Mathematical Modeling of the transport and dissolution of citrate-stabilized silver nanoparticles in porous media. Environmental Science & Technology. https://doi.org/10.1021/es400692r 130719135526002.

Tolaymat, T.M., El Badawy, A.M., Genaidy, A., Scheckel, K.G., Luxton, T.P., Suidan, M., 2010. An evidence-based environmental perspective of manufactured silver nanoparticle in syntheses and applications: a systematic review and critical appraisal of peer-reviewed scientific papers. Sci. Total Environ. 408, 999–1006. https://doi.org/10.1016/j.scitotenv.2009.11.003.

Tripathi, S., Champagne, D., Tufenkji, N., 2012. Transport behavior of selected nanoparticles with different surface coatings in granular porous media coated with Pseudomonas aeruginosa biofilm. Environ. Sci. Technol. 46, 6942–6949. https://doi.org/10.1021/es202833k.

Turkevich, J., Stevenson, P.C., Hillier, J., 1951. A study of the nucleation and growth processes in the synthesis of colloidal gold. Discussions of the Faraday Society 11, 55–75.